Exact ground states of the Kaya-Berker model

Sebastian von Ohr and Alexander K. Hartmann*
Institute of Physics, Carl von Ossietzky University, 26111 Oldenburg, Germany

(Received 17 October 2017; revised manuscript received 23 March 2018; published 6 July 2018)

Here we study the two-dimensional Kaya-Berker model, with a site occupancy p of one sublattice, by using a polynomial-time exact ground-state algorithm. Thus, we were able to obtain $T = 0$ results in exact equilibrium for rather large system sizes up to 777^2 lattice sites. We obtained the sublattice magnetization and the corresponding Binder parameter. We found a critical point $p_c = 0.64(1)$ beyond which the sublattice magnetization vanishes. This is clearly smaller than previous results which were obtained by using nonexact approaches for much smaller systems. For each realization we also created minimum-energy domain walls from two ground-state calculations, for periodic and antiperiodic boundary conditions. The analysis of the mean and the variance of the domain-wall energy shows that there is no thermodynamic stable spin-glass phase at nonzero temperature, in contrast to previous claims about this model. For large values of p, the standard deviation of the domain-wall decreases with the system size like a power law with exponent roughly $\theta \simeq -0.1$, which is different from the standard two-dimensional Ising spin glass where $\theta \simeq -0.29$.

DOI: 10.1103/PhysRevE.98.012108

I. INTRODUCTION

Compared to regular or pure systems, magnetic systems with quenched disorder, like spin glasses and random-field systems [1], exhibit many peculiar properties. Their complex low-temperature behavior is still not fully understood, even for two-dimensional systems. Because analytical solutions are not available, computer simulation studies [2] are often performed. With respect to Markov-chain Monte Carlo simulations [3], one of the difficulties is their slow glassy dynamics, resulting in very long equilibration times. Other approaches to study spin-glasses involve finding and characterizing ground states [4,5]. In three or more dimensions, only algorithms with exponential running time are known, but in two dimensions polynomial-time algorithms are available.

One of the interesting differences between two-dimensional (2D) and three-dimensional (3D) spin glasses is that so far all 2D models with finite-range interactions show a transition only at $T = 0$ [6–13]. At all finite temperatures the spin-glass phase vanishes for 2D models. In contrast 3D models have a nonzero transition temperature above. This spawned the search for 2D models with a finite critical temperature. One such candidate is the Kaya-Berker model [14], which was claimed to exhibit a spin-glass-like phase for nonzero temperatures, i.e., a phase transition at a finite temperature. This claim was based on numerical studies of rather small systems with nonexact algorithms. Here, we will present results for this model which we obtained by using exact and fast ground-state algorithms. This allowed us to study rather large systems with more than 10^5 spins in exact equilibrium. Our result strongly suggest that in contrast to previous claims, the model does *not* exhibit a low-temperature spin-glass phase.

This paper is organized as follows: We first introduce the model along with suitable measurable quantities and review previous results. Next, we outline the algorithm we use to obtain exact ground states and, by changing the boundary conditions, to obtain domain-wall (DW) energies. In the main part, we present our results, followed by our conclusions.

II. MODEL

The Kaya-Berker model [14] is a variation of the Ising model on a two-dimensional triangular lattice with $N = L_x \times L_y$ spins. The spins s_i take the values ± 1 and all bonds are antiferromagnetic. Its Hamiltonian is given by

$$\mathcal{H} = -J \sum_{\langle i,j \rangle} \epsilon_i s_i \epsilon_j s_j, \tag{1}$$

with $J < 0$ and $\langle i,j \rangle$ indicating a sum over all nearest-neighbor pairs. The model allows for dilution, which is described by the quenched disorder variables $\epsilon_i \in \{0,1\}$. Every spin is located on one of three sublattices, such that every spin has only neighbors in the two other sublattices. Figure 1 shows the triangular lattice and subdivision into three sublattices. Here, one of the sublattices is diluted and only a fraction p of spin sites is occupied ($\epsilon_i = 1$), while a fraction $1 - p$ of sites is not occupied by a spin ($\epsilon_i = 0$). The other two sublattices are not diluted.

In the fully occupied $p = 1$ case, every triangle of spins is frustrated. This special configuration was solved exactly [15,16], with the result that the system is disordered at all temperatures. Ground states are characterized by exactly one-third of unsatisfied bonds. While there are some configurations that are ordered, e.g., alternating rows of all up-spins with row of all down-spins, no energy advantage is obtained for long-range order. Because of entropic dominance, i.e., the exponential dominance of these non-ordered ground-state configurations, no long-range order occurs.

*a.hartmann@uni-oldenburg.de

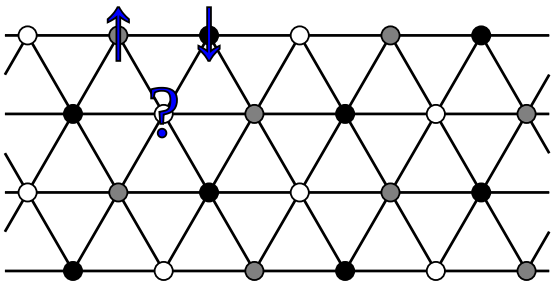

FIG. 1. 6×4 triangular lattice showing the subdivision into the three sublattices, as indicated by the three colors of the nodes (white, gray, black). Every triangle is frustrated, since not all bonds can be satisfied.

For the diluted $p = 0$ case, one obtains a honeycomb lattice, where the frustration is fully relieved. The ground state (GS) is ordered and spins are aligned antiparallel with all of their neighbors. Within the two remaining sublattices spins in the same sublattices are aligned in the same direction.

By choosing an intermediate value of p, the number of frustrated plaquettes can be varied. The behavior of the system is complicated and allows for interesting behavior. These intermediate values of p result in a ground state with zero magnetization on the diluted lattice and roughly equal but opposite magnetization on the two undiluted lattices. The order parameter is therefore defined as the per-lattice magnetization

$$m_\alpha = \frac{1}{N_\alpha} \sum_{i \in \alpha} \epsilon_i s_i, \tag{2}$$

with $\alpha = a,b,c$ denoting one of the three sublattices and $N_\alpha = \sum_{i \in \alpha} \epsilon_i$ being the number of spins of sublattice α. The diluted lattice will be lattice a.

A model similar to the Kaya-Berker model with uniform dilution in all sublattices [17–20] was studied earlier. While the first study observed spin-glass behavior, all later publications argue against a spin-glass phase. However, they found a large but finite correlation between spins, which could be mistaken for long-range order in small systems. In 2000, Kaya and Berker devised the aforementioned model, which notably differs from the older model by restricting the dilution to one sublattice [14]. The authors studied it by using hard-spin mean-field (HSMF) theory. For HSMF, each spin s_i not only interacts with its neighbors s_j through its mean spin values m_j as in standard mean-field theory. Instead, the self-consistent equation for the site-dependent mean values m_j involves a sum over all possible 2^n configurations of the n neighbors such that each spin orientation $s_j = \pm 1$ occurs with a probability which is compatible with its mean value m_j. As a further approximation, in Ref. [14] the disorder average is performed and the site dependent mean values are replaced by their sublattice mean values, resulting in three coupled equations. For the sublattice spin-glass order parameter (which involves again the site-dependent mean values),

$$q_\alpha = \left[\frac{1}{N_\alpha} \sum_{i \in \alpha} (m_i - m_\alpha)^2 \right]^{1/2}, \tag{3}$$

they found nonzero values at finite temperatures for occupancy $p < 0.958$. However, their study involves only small system with sizes up to 30×30 and features no finite-size scaling analysis. Other studies analyzed the Kaya-Berker model by using Monte Carlo (MC) simulations [21,22], effective-field theory (EFT) [23], and a modified pair-approximation (PA) method [24]. The EFT approach is based on a cluster approximation with clusters comprised of only a single spin and interactions with their nearest neighbors [25], which is quite similar to HSMF. The PA method is based on the cumulant expansion of the entropy. So far, none of the studies found conclusive evidence in favor for or against the spin-glass phase at finite temperatures. Note that, when using MC simulations, the system certainly appears to behave like a glassy system in the range of accessible system sizes and timescales. Simulations at a large range of system sizes, and proof of proper equilibration, would be needed, which is difficult and requires a huge numerical effort for glassy systems.

This work aims to settle this open question by using an exact ground-state algorithm which allows us to investigate large systems in equilibrium. Studying exact ground states allows one to calculate domain-wall energies, which are often used [6,7,11,26–28] to verify the stability of a phase at finite temperatures. In the following section we explain our numerical approaches.

III. ALGORITHM

The GS algorithm is taken from Ref. [29] where it is used to calculate ground states of the 2D random bond Ising model on a planar triangular lattice. Here we present only a short summary of the algorithm, which is visualized in Fig. 2.

We start with a given realization of our system, for which we want to calculate a GS. Lattice sites and bonds are interpreted as the nodes and edges of a weighted undirected graph G. The weights are given by the strength of the bonds. For this model, if $J = 1$, all weights are set to -1, but the algorithm is suitable for arbitrary weights. Here we consider periodic boundary conditions in the horizontal (x) direction and open boundary conditions in the vertical direction. This means that we study the model on a lattice with a planar structure, which is a prerequisite for the algorithm [30]. The periodic boundary conditions in one direction are needed to introduce domain walls to the system; see below. On the other hand, if we had periodic boundary conditions in both directions, the lattice would still be two dimensional but would not be planar any more, so the algorithm would not be applicable. Now, from the given interaction graph, we construct an auxiliary graph G', by starting with the dual graph of the undiluted triangular lattice, i.e., G' is a hexagonal (honeycomb) graph. Next we add two additional rows of each $2L_x$ vertices at the top and bottom, respectively. The resulting graph contains a total of $(2L_x) \times (L_y + 1)$. Since the $2L_x \times (L_y - 1)$ faces in G are separated by single edges, there is a corresponding dual edge in G' for every edge in G. Each dual edge basically "crosses" the corresponding edge from G. These edges carry the same weight as the corresponding edges in G. We use the *edges* in G' to model the *site* dilution by setting the weight to zero for edges which are adjacent to unoccupied sites. Also, the additional edges in G', i.e., all the edges at the top and bottom, which do not correspond to an edge in G, are assigned zero weight.

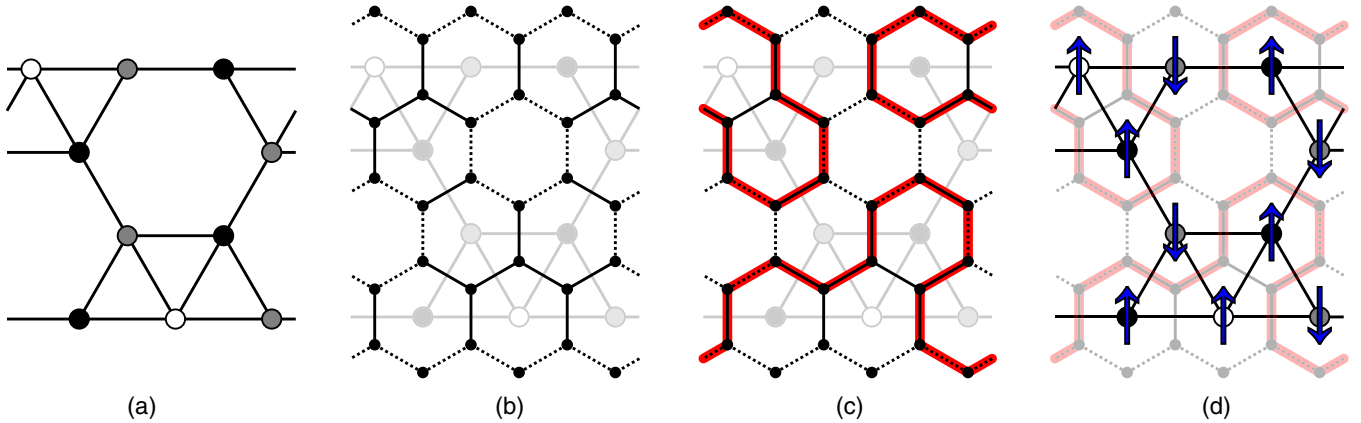

FIG. 2. Illustration of steps involved in ground-state calculation. The sample shows a 3×4 system with periodic boundary conditions in the horizontal direction. (a) Initial system with $p = 0.5$ occupation on the white sublattice. (b) Construction of the dual graph of the original undiluted system with additional vertices and edges at the top and bottom. Edges that do not correspond to edges in the diluted system carry zero weight and are marked by using stroked lines. (c) Set of minimal weighted loops on the dual graph. These paths separate clusters of aligned spins. (d) Ground state constructed by setting the top left spin to *up* and assigning all remaining spins using the clusters determined earlier.

In the next step, a set of closed nonintersecting loops with minimum edge weight are calculated. Calculating this set is part of the negative-weight percolation [31] problem, which yields a globally optimal solution. This works by transforming the problem into a *minimum-weight perfect matching problem* which is a standard problem in graph theory and can be solved exactly in a time growing only polynomially with system size. Note that, while the total edge weight of the whole set of loops is optimized, each individual loop has a total negative or zero weight. These loops separate clusters of aligned spins that form a GS of the system. Suppose two spins share a bond that favors antiparallel alignment, then the corresponding edge in G' that separates these spins carries a negative weight. Because we look for minimal weighted loops, this edge is likely to be included in one of the loops and thus the spins are in different clusters, fulfilling the antiparallel alignment of the bond. In general, the weight of a loop is the negative of the energy of the DW surrounding the spins inside the loop. Therefore, by flipping the spins inside a loop, the total energy will be decreased by twice this amount.

Given this, the last step of the algorithm is to construct a ground state from the minimal weighed loops. This is achieved by setting the top left spin to some value, e.g., *up*. The orientation of neighboring spins can then be determined by looking at the loops. If spins are separated by a loop they need be aligned in opposite direction. This process is repeated until all spin have been assigned an orientation. Since there is no external field, the configuration obtained by flipping all spins is also a GS of the system.

From the calculated GS, we can easily obtain the magnetization values of the sublattices. Nevertheless, due to the discrete structure of the model, the GS is highly degenerate. Since the ground states have all the same Boltzmann weight, one would like to sample uniformly from the ground states. Nevertheless, the algorithm is not random and returns always the same ground-state configuration when rerun for the same realization of the disorder. Therefore, we used a small randomization of the bonds to lift the degeneracy. Instead of the original bond values $J_{i,j} = 0, -1$, we used

$$\hat{J}_{i,j} = S J_{i,j} + X_{i,j}, \tag{4}$$

with a constant scaling factor S and uniform distributed discrete random variables $X_{i,j} \in \{-V, -V+1, \ldots, V-1, V\} \subset \mathbb{Z}$. The values $S = 10^6$ and $V = 100$ are used throughout the remaining analysis. The large scaling factor is used to keep the bond strength an integer, while allowing for slight variations such that the ground state of the modified system is also a GS of the original system, for each realization. Although this randomization does not guarantee a uniform sampling of the ground states, it was shown [32] that, for the two-dimensional random-bond Ising model, the influence of the bias is very weak such that the results are reliable within the statistical error bars.

Furthermore, we also studied the scaling of domain-wall (DW) energies. Here, DWs separate regions of spins which exhibit relative to each other GS orientation, while across the DWs, their relative orientation is opposite to the GS. The DWs are induced [6–9,11] for a given realization by first calculating the GS for the original system, leading to a ground state energy E_{p}. Another GS is obtained for a modified system, which typically results in creating domain walls, as depicted Fig. 3. Here, the second GS with energy E_{ap} is calculated for a system, where the boundary conditions are switched from periodic to antiperiodic in the horizontal direction. The switch of the boundary conditions is realized by inverting the sign of the bonds in one (top-bottom) column of bonds. Note that for the original ground-state configuration, the change of the boundary conditions leads to an increase of the energy of order $O(L)$. Therefore it is typically energetically favorable for the second GS that the relative orientations of the spins across this column of bonds switches, creating a top-down domain wall. This happens if there exists anywhere a second top-down domain wall with an energy cost smaller than the hypothetical energy cost of leaving the relative orientation of the spins across the column of bonds unchanged. Since the second domain wall has the freedom to run everywhere, such a

FIG. 3. Illustration of a domain wall generated by switching the boundary conditions. This is equivalent to changing the signs of all bonds in one (top-down) column (vertical gray-black interface). This leads typically to the flip of a domain of spins (black) with respect to the original ground state (gray). The (left) linear domain wall, located at the column of flipped bonds, is trivial, does not lead to an energy change, and is not shown below.

"low-cost" domain wall will typically exist. Hence, due to the periodic boundary conditions in the x direction, for the second GS a domain of spins between the column of flipped bonds and the second domain wall will be flipped with respect to the first GS. The energy of the (second) domain wall is given by

$$\Delta E = E_{\mathrm{p}} - E_{\mathrm{ap}}. \tag{5}$$

If the disorder-averaged value $\langle \Delta E \rangle$ increases with system size, domain walls become more and more expensive, thus an ordered state with nonzero order parameter m_α is stable. On the other hand, if $\langle \Delta E \rangle$ decreases with system size, for large systems arbitrary small thermal fluctuations will be sufficient to destroy an ordered state, which means $T_{\mathrm{c}} = 0$. Nevertheless, a nonmagnetized state might exhibit spin-glass order. This is signified by a growth of the width $\sigma(\Delta E)$ of the (disorder) distribution of domain-wall energies when increasing the system size L, while the average $\langle \Delta E \rangle$ decreases [7,33]. Equivalently to the width, one could monitor the size dependence of the average $\langle |\Delta E| \rangle$ of the absolute value of the domain-wall energy. Below, we will use this approach to show that for $p < p_{\mathrm{c}} \simeq 0.64$ the Kaya-Berker model exhibits indeed a global antiferromagnetic order, which is equivalent to a ferromagnetic order for the fully occupied sublattices. We will also show that our data is compatible with the absence of nontrivial spin-glass order at nonzero temperature for all values of p.

IV. RESULTS

To obtain the following results, between 5000 and 10 000 random realizations of the disorder for the Kaya-Berker model were studied for various system sizes, for many values of the disorder parameter p. We studied square systems $L = L_x = L_y$ with $L \in [30,345]$. For each realization we calculated exact ground states of the system with periodic and antiperiodic boundary conditions, respectively. Each realization and both GSs were saved to disk and analyzed later. All systems have open boundary conditions in the y direction, since the GS algorithm cannot handle periodicity in both directions. This does not impact the ordering of the system, because the change of boundary conditions, to induce a domain wall, is performed perpendicular to the open boundary condition. The DW therefore spans the system between the open boundaries.

First the magnetization of the Kaya-Berker model in the ground state is studied. The sublattice magnetizations defined in Eq. (2) are calculated as per a function of the fraction of occupied spins p. The sign of the sublattice magnetization is chosen such that the magnetization for lattice b is always positive. One problem with calculating GSs is that most observables depend on the specific GS that is generated. The discrete nature of the Kaya-Berker model results in an exponential GS degeneracy. This means that there are many GSs, all sharing the same energy, but varying in other properties. The way the algorithm constructs the matching, and thus a GS, is not statistically controlled. Thus, it could be that certain "types" of GS are favored by the construction. Here, we found (not shown) that the GS calculated by the algorithm has a systematic tendency towards small sublattice magnetization within the set of all degenerate GSs. This could lead to slightly biased results for all quantities related to the magnetization. The GS degeneracy can be broken by slightly randomizing the bonds, such that the GS is unique but the obtained configuration is still a GS of the original system. In this way one GS will be sampled randomly from all degenerate GSs. In a past study [32] it was shown that this procedure successfully removes (at least within statistical error bars) any bias. For this reason, we used for all results concerning the magnetization the randomized, i.e., randomly sampled, GSs. The size of the randomization was chosen as large as possible under the constraint that, for the largest system, all sampled states are still ground states of the original Hamiltonian. Generally, different ground states differ by clusters of flipped spins. Hence, the states of the *bonds*, which determine the energy of a configuration, change only at the domain walls. For smaller systems, where the possible domain walls are shorter, the randomization is even less likely to lead to non-ground-state configurations. Therefore the same strength of the randomization can be used for smaller systems. Please note that the degenerate ground states have by definition all the same energy. Thus for the results concerning the domain-wall energies (see below), no uniform sampling is needed in principle and the original ground-state energies must be used. This means, for any spin configuration, the energy is evaluated by using the unperturbed Hamiltonian.

The results for the magnetization of sublattice b are shown in Fig. 4. For small values of p the magnetization is high, while near $p = 0.64$ it decreases strongly towards zero. This shape is typical for systems exhibiting ordered-disordered phase transitions. The curves for different system sizes decrease strongly near $p = 0.62$ (interestingly, they cross near $p = 0.642$) and become very small for larger values of p, which indicates a phase transition. Note that for the case of the unsampled ground states (without randomization), which have strong bias towards smaller magnetization, the curves (not shown here) cross near $p = 0.639$. This moderate difference indicates that the influence of the possibly not completely uniform GS sampling on the transition is rather small and even without any sampling of the GSs the determination of the transition point would be rather precise, in particular relative to the previous results obtained in the literature [14].

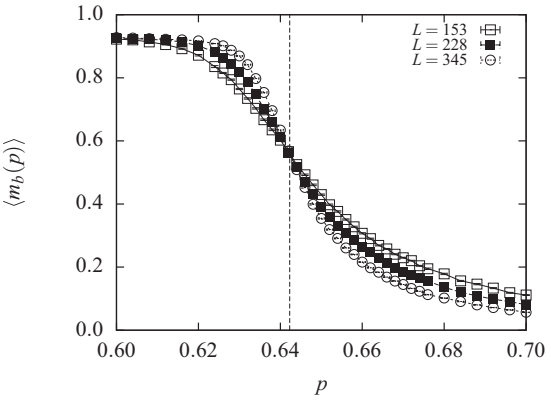

FIG. 4. Magnetization of sublattice b at different fractions p of occupied sites and system sizes L. The magnetization was obtained for each disorder realization from a randomly sampled state among the degenerate GSs.

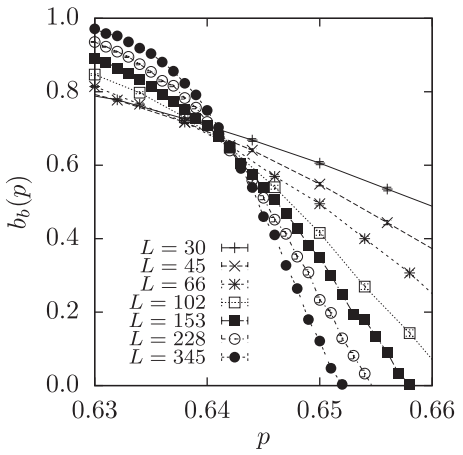

FIG. 5. Binder parameter of sublattice b as a function of the sublattice occupancy p, for different system sizes.

Next, as usually done for second-order phase transitions, the critical point is determined more precisely by performing a finite-size scaling analysis of the Binder parameter [34]

$$b_\alpha = \frac{1}{2}\left(3 - \frac{\langle m_\alpha^4\rangle}{\langle m_\alpha^2\rangle^2}\right). \tag{6}$$

When plotting b as a function of the disorder parameter p, the curves for different system sizes L will intersect (for large enough system sizes) at the critical point p_c where the sublattice ferromagnetic (global antiferromagnetic) order disappears. This allows for a convenient determination of the critical point. Furthermore, finite-size scaling [35] shows that, when rescaling the p axis according to $(p - p_c)L^{1/\nu}$, for the correct value of p_c and a suitably chosen value of ν, the data will collapse onto a single curve. More precisely, the Binder parameter follows

$$b(p, L) = \tilde{b}((p - p_c)L^{1/\nu}), \tag{7}$$

where $\tilde{b}(\ldots)$ is a non-size-dependent function of one scaled variable. The quantity ν is a *critical exponent* which describes the divergence of the correlation length when approaching a second-order phase transition. The actual value of ν (together with other critical exponents) allows us to classify second-order phase transitions according to *universality classes*.

The results for the Binder parameter and the best data collapse, as obtained from the *autoscale script* [36], are shown in Figs. 5 and 6. The x range of the collapse was restricted to $[-0.75, 0.25]$, which gave the best collapse quality of $S = 1.17$. S describes the mean-squared fluctuation of the data along the collapse curve measured in *autoscale* in terms of error bars. The system sizes $L = 30$ and $L = 45$ were excluded from the data collapse, since they deviate from the other curves and resulted in a worse collapse. This is because of their quite small system size, which would require corrections to scaling to match the other curves. From this analysis we find that the Kaya-Berker model has a critical point of $p_c = 0.6423(3)$. This error bar is purely statistical. Since we have seen that the bond randomization may have some small influence and because we obtained a crossing of the magnetization without GS sampling at roughly 0.639 we only quote as final result:

$$p_c = 0.64(1). \tag{8}$$

This result is much smaller than any of the previous results of $p_c = 0.958$ by Kaya and Berker [14], $p_c \approx 0.95$ by using a Monte Carlo simulation [21], or $p_c = 0.875$ obtained by using effective-field theory (EFT) [23]. However, the discrepancy can be explained by taking a closer look at the previously used methods. First, the results by Kaya and Berker are obtained by HSMF theory. This method includes several approximations, like the mean-field nature of the approach and the partial use of locally averaged magnetizations. Furthermore, this method includes a form of stochastic iteration. These iterations often get stuck in local minima. In fact, the authors found a multiplicity of solutions and used only the most stable set to determine the critical point. Other not-so-stable solutions are fragmented and show a much lower magnetization than the stable one. Indeed the solution with the lowest magnetization looks like it could become zero somewhere around $0.6 < p < 0.7$, which would coincide with our $p_c = 0.64(1)$ result. The other result obtained by Monte Carlo (MC) simulations also suffers from the problem that the dynamics of the Kaya-Berker model

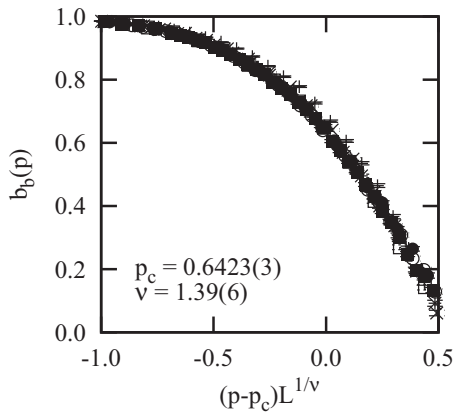

FIG. 6. Rescaled Binder parameter with a rescaled p axis using the appropriate scaling variables $p_c = 0.6423(3)$, $\nu = 1.39$.

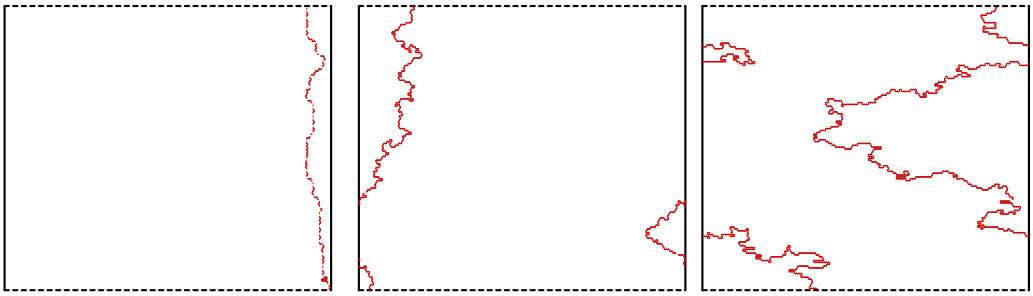

FIG. 7. Exemplary domain walls at different occupancy. The solid and dashed border marks periodic and open boundary conditions, respectively. The occupancy was set to $p = 0.2$ (left), $p = 0.6$ (center), and $p = 0.8$ (right).

becomes very slow at low temperatures and often also gets stuck in local energy minima. Finally, the other approaches, which are very similar to the further approximation of HSMF, impose also sublattice-wise uniformity of the magnetization. This restriction may not capture the whole behavior of the model, leading to wrong results. Therefore, the exact-GS approach which we used here is much more reliable than any of the previous results since it neither includes approximations nor does it suffer from convergence problems. Finally, we can treat much larger sizes compared with the previous approaches.

We also determined an estimate $\nu = 1.39(6)$ for the value of the critical exponent of the correlation length. No corresponding result for the Kaya-Berker model for this critical exponent at the $T = 0$ antiferromagnet-paramagnet transition is known to us from the literature. Thus a direct comparison is not possible. Nevertheless, for the random-bond Ising model, which exhibits a ferromagnet-paramagnet transition (with spin-glass behavior at exactly $T = 0$), a value $\nu = 1.55(1)$ was found [32]. This is not fully compatible, but only two error bars away from the value obtained here. Therefore, the transitions might be in the same universality class.

Next, the domain-wall length l is studied. This is another property which strongly depends on the specific GS of a given realization. As explained above, DWs are obtained by calculating the GS of a realization, flipping the boundary condition, calculating a new GS, and comparing the two obtained GSs. Note that the bond randomization is again used, which should result in typical domain wall lengths among many possible degenerate DWs. The influence of the bond-randomization is less clear here. The reason is that the original algorithm does not have a tendency to favor specific domain-wall lengths, in contrast to the sublattice magnetization where low magnetizations seem to be preferred. More details and a more sophisticated method to determine shortest and maximal length domain walls are presented in Ref. [37]. Nevertheless, the present approach is sufficient for our purpose, because the results presented concerning the domain walls are not fundamental for our conclusions. Anyway, the domain-wall results, see below, are compatible with the determination of the transition point obtained from the magnetization and from the domain-wall energy. This analysis uses 10^4 samples for each system size $L \in [30,777]$ and occupancy value p. Some exemplary domain walls at different occupancy p are shown in Fig. 7. For small values of p, where the GS is ordered, the DWs are very straight. With increasing value of p the domain walls exhibit a higher fractal dimension.

The measured averaged lengths l of the DWs are shown in Fig. 8 as a function of the system size L. All of the data sets show a clean power-law behavior of the form

$$l(L) \sim L^{d_f}. \tag{9}$$

where d_f is the fractal exponent which depends on p. A power-law fit was performed for all data sets, excluding the small system sizes $L < 50$. The fits match the data sets very well. The resulting fractal dimension d_f (see Fig. 9) exhibits a change between the $p \leqslant 0.65$ and $p \geqslant 0.70$ data sets visible as a rather sharp jump in the plot. Apart from this sharp jump,

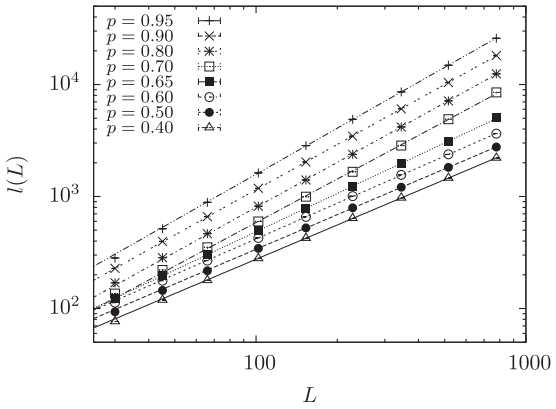

FIG. 8. Domain-wall length l at different system sizes L. The straight lines are power-law fits to the data sets.

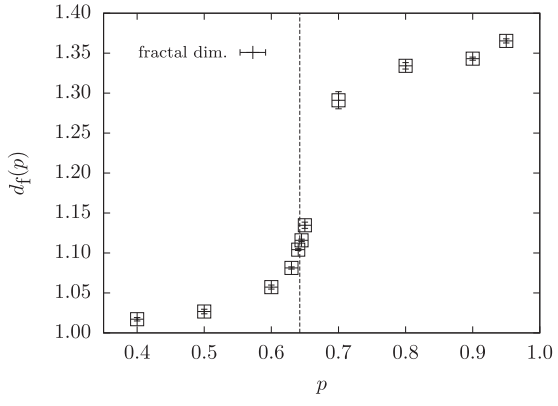

FIG. 9. Fractal dimension d_f of the domain-wall length at different occupancy p. The vertical dashed line marks the critical point $p_c = 0.64(1)$.

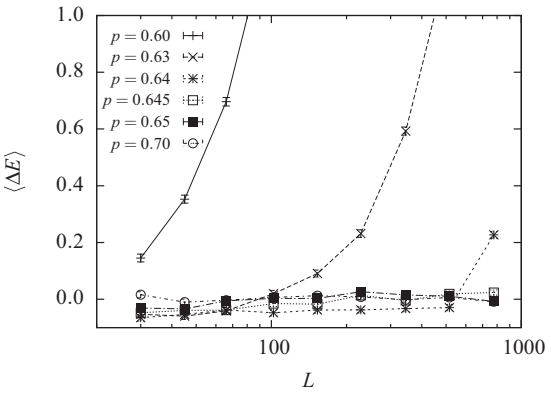

FIG. 10. Average domain-wall energy at different system sizes. Data points are connected by using straight lines for better visibility.

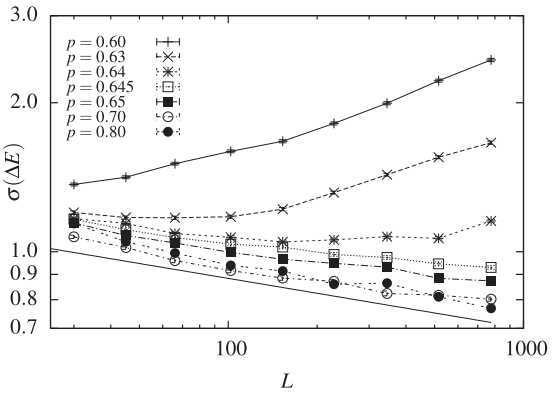

FIG. 11. Standard deviation of domain-wall energy at different system sizes. Data points are connected by using straight lines for better visibility. The straight solid line shows a power law $\sim L^{-0.1}$ for comparison.

the fractal dimension also grows slowly with the occupancy. By interpolating between the two values closest to the critical point at $p = 0.64$ and $p = 0.645$, the fractal dimension at the critical point is $d_f = 1.109(2)$. This value is different from the value $d_f = 1.222(1)$ obtained for the 2D random-bond Ising model on a triangular lattice [29] and also on a square lattice [38].

Finally, the results of the DW energy calculations are presented. This enables us to discuss one of the central issues of the paper, whether there exists a stable spin-glass phase in the model at $T > 0$. The same 10^4 samples used for the domain-wall length are analyzed here. The GS energy values are calculated by using the spin configurations and the original unperturbed bond values. Hence, the energy is the same for all degenerate ground states. Therefore, the randomization has no influence on the results. These results are visualized in Fig. 10 and used to investigate the main question whether there exists a spin-glass phase at $T > 0$ in this model. The data are plotted on a semilog scale, since some average values are negative. For occupancy $p < 0.645$ the average DW energy increases linearly. This includes values of $p < 0.6$ which were omitted from the plot for a clearer image. This indicates a sublattice ferromagnetic, i.e., globally antiferromagnetic, phase. This becomes visible because the introduction of a DW breaks the long-range order but costs energy. This behavior is expected for occupancy smaller than the critical point p_c, since the system is antiferromagnetic at $p = 0$. For $p \geqslant 0.645 \simeq p_c$ the DW energy is roughly zero, which is typical for both possibilities of a paramagnetic and a spin-glass phase. Note that fairly large system sizes are required, because the $p = 0.63$ curve is also approximately zero at first, but then increases around $L = 100$. Similarly, the $p = 0.64$ curve only deviates from zero around $L = 600$. This means that systems around these occupancy values may appear not sublattice ferromagnetically ordered at small system sizes. From the analysis of the magnetization we know that, beyond p_c, no (anti-)ferromagnetic order exists, therefore it is clear that for values $p > p_c$ the DW energy will not rise as a function of the system L.

To determine whether there exists a spin-glass phase, we look at the standard deviation of the DW energy in Fig. 11. A spin-glass phase corresponds to a mean domain-wall energy of zero and to a growth of the standard deviation [33]. This can be understood because the domain-wall energy can be seen as an effective coupling constant for a block spin of size L. Thus, in a corresponding real-space renormalization transformation of the distribution of couplings, a distribution which remains centered at zero but grows in width corresponds to a growth of the "glassiness." On the other hand, a convergence of the distribution of couplings to a zero mean and zero width describes a vanishing of the couplings at large scales, i.e., a paramagnetic phase. This approach of studying mean and standard deviation of domain-wall energy has been used already for several disordered models to determine whether a spin-glass phase exists, which is typically not the case in two dimensions [7,9,11–13,32,33,39], but is the case for higher dimensions [6,26,40–42].

For the present model, the curves split into two categories: Increasing standard deviation with the system size at $p < 0.645$, where the mean increases and decreasing values at $p \geqslant 0.645$, where the mean is close to zero. This parallel behavior of standard deviation and mean makes it also unlikely that, at much larger sizes, the standard deviation will grow again for some values $p > p_c$. Nevertheless, this cannot be completely excluded, because it is the case for any numerical study which is always limited in system size. Note that, for $p > p_c$, the standard deviation follows roughly a power-law behavior, which is typical for this quantity. The exponent, usually denoted θ, seems to be close to $\theta = -0.1$, as indicated by a straight line in the plot [we obtained an exponent of $-0.09(1)$ when fitting the data for $p = 0.7$ and an exponent of $-0.11(1)$ for $p = 0.8$]. This is clearly different from the standard two-dimensional Ising spin glass where a value of $\theta \simeq -0.29$ [11,39,42] has been obtained. Therefore, the Kaya-Berker model might be in a different universality class.

To sum up, these results suggest that the ferromagnetic phase is stable at finite temperatures for $p < p_c$ because the mean domain-wall energy grows with system size in this range. Nevertheless, the claimed spin-glass phase only exists at $T = 0$, because there exists no range of p values where the mean domain-wall energy is zero (or converges to zero) and at the same time the standard deviation increases with system size. Thus, for $p > p_c$, where both mean and standard deviation of the DW energy converge to zero, there exists only

a paramagnetic phase at $T > 0$. Hence, it can be concluded that previous reports of a stable $T_c > 0$ spin-glass phase are not supported by our results.

V. CONCLUSIONS

We have numerically studied the Kaya-Berker model with a site occupancy p of one sublattice by using an exact ground-state algorithm. Thus, we were able to obtain $T = 0$ results in exact equilibrium. Since the ground-state calculation is equivalent to obtaining a minimum-weight perfect matching, it is possible to obtain ground states with a running time growing only polynomially in system size. Therefore, we were able to study very large system sizes of up to a total number of $\sim 10^5$ lattice sites, i.e., laterally up to $L = 777$. This is much larger than in the previous work on this model.

From the obtained GSs, we calculated the magnetization and the corresponding Binder parameter as a function of the occupancy p. Here we used a slight randomization of the bonds to obtain an almost unbiased sampling of the degenerate ground states. From the Binder parameter, we obtained a critical value $p_c = 0.64(1)$ where the sublattice magnetization vanishes. This value is considerably smaller than previous results. Nevertheless, the previous results were obtained by using methods which involve approximations, nonequilibrium sampling often without a guarantee of convergence and they were restricted to small system sizes. Therefore, our results are much more reliable than those obtained from the previous studies. Although there might be a slight bias from the sampling of the ground states, we know from the previous results for the random bond (spin-glass) model that its influence is very small. Also, we checked that when using the nonsampled ground states, which have a clear tendency towards smaller magnetizations, the obtained transition point changes only in the third digit.

We also studied domain walls which are obtained by comparing the GS of the original realizations with periodic boundary conditions in the x direction and the GS of the realization with antiperiodic boundary conditions. By analyzing the length of the domain walls and its dependence on the system size, we obtained the fractal dimension d_f. Looking at the fractal dimension d_f as a function of p supports the results for phase transition obtained by analyzing the magnetization. In the phase where the sublattice magnetization is nonzero, we obtained basically $d_f = 1$. Close to the critical point, a strong increase of d_f can be observed.

The results for the scaling of the average DW energy, where the sampling procedure of the degenerate GSs has no influence at all, are also compatible with a transition at the location p_c where the magnetization vanishes. The standard deviation of the DW energy distribution changes from growing to shrinking with system size L at (or close to) the same point p_c. Thus, it is rather likely that the Kaya-Berker model does not exhibit a spin-glass phase at a low but finite temperature, because this would have to go together with a decrease of the mean value and an increase of the standard deviation with the system size for some values of p. For the power-law exponent describing the behavior of the standard deviation of the DW energy, we obtained a value of $\theta \simeq -0.1$ for $p > p_c$, which is clearly different from the value of -0.29 established for the standard two-dimensional Ising spin glass.

To conclude, opposite some claims to the contrary, up to now no two-dimensional random frustrated Ising system has been found with a finite-temperature spin-glass phase. It still remains an open question whether such a system exists, but it appears to us to be unlikely.

ACKNOWLEDGMENTS

We thank A. Peter Young and Hendrik Schawe for critically reading the manuscript. The simulations were performed on the HPC clusters HERO and CARL of the University of Oldenburg jointly funded by the DFG through its Major Research Instrumentation Program (INST 184/108-1 FUGG and INST 184/157-1 FUGG) and the Ministry of Science and Culture (MWK) of the Lower Saxony State.

[1] *Spin Glasses and Random Fields*, edited by A. P. Young (World Scientific, Singapore, 1997).
[2] A. K. Hartmann, *Big Practical Guide to Computer Simulations* (World Scientific, Singapore, 2015).
[3] M. E. J. Newman and G. T. Barkema, *Monte Carlo Methods in Statistical Physics* (Oxford University Press, Oxford, 1999).
[4] A. K. Hartmann and H. Rieger, *Optimization Algorithms in Physics* (Wiley-VCH, Weinheim, 2001).
[5] *New Optimization Algorithms in Physics*, edited by A. K. Hartmann and H. Rieger (Wiley-VCH, Weinheim, 2004).
[6] W. L. McMillan, Phys. Rev. B **30**, 476 (1984).
[7] A. J. Bray and M. A. Moore, J. Phys. C: Solid State Phys. **17**, L463 (1984).
[8] L. Saul and M. Kardar, Phys. Rev. E **48**, R3221 (1993).
[9] H. Rieger, L. Santen, U. Blasum, M. Diehl, M. Jünger, and G. Rinaldi, J. Phys. A: Math. Gen. **29**, 3939 (1996).
[10] J. Houdayer, Eur. Phys. J. B **22**, 479 (2001).
[11] A. K. Hartmann and A. P. Young, Phys. Rev. B **64**, 180404 (2001).
[12] A. C. Carter, A. J. Bray, and M. A. Moore, Phys. Rev. Lett. **88**, 077201 (2002).
[13] A. K. Hartmann, Phys. Rev. B **67**, 214404 (2003).
[14] H. Kaya and A. N. Berker, Phys. Rev. E **62**, R1469 (2000).
[15] G. H. Wannier, Phys. Rev. **79**, 357 (1950).
[16] R. M. F. Houtappel, Physica **16**, 425 (1950).
[17] G. S. Grest and E. F. Gabl, Phys. Rev. Lett. **43**, 1182 (1979).
[18] J. A. Blackman, G. Kemeny, and J. P. Straley, J. Phys. C: Solid State Phys. **14**, 385 (1981).
[19] C. Z. Andérico, J. F. Fernández, and T. S. J. Streit, Phys. Rev. B **26**, 3824 (1982).
[20] H.-L. Tang, Y. Zhu, G.-H. Yang, and Y. Jiang, Phys. Rev. E **81**, 051107 (2010).
[21] M. D. Robinson, Master's thesis, The University of Maine, 2003, https://digitalcommons.library.umaine.edu/etd/317/.

[22] M. D. Robinson, D. P. Feldman, and S. R. McKay, Chaos **21**, 037114 (2011).
[23] M. Žukovič, M. Borovský, and A. Bobák, J. Magn. Magn. Mater. **324**, 2687 (2012).
[24] T. Balcerzak, K. Szałowski, M. Jaščur, M. Žukovič, A. Bobák, and M. Borovský, Phys. Rev. E **89**, 062140 (2014).
[25] M. Žukovič, M. Borovský, and A. Bobák, Phys. Lett. A **374**, 4260 (2010).
[26] A. K. Hartmann, Phys. Rev. E **59**, 84 (1999).
[27] C. Amoruso, E. Marinari, O. C. Martin, and A. Pagnani, Phys. Rev. Lett. **91**, 087201 (2003).
[28] F. Romá, S. Risau-Gusman, A. J. Ramirez-Pastor, F. Nieto, and E. E. Vogel, Phys. Rev. B **75**, 020402 (2007).
[29] O. Melchert and A. K. Hartmann, Comput. Phys. Commun. **182**, 1828 (2011).
[30] A. K. Hartmann, in *Rugged Free Energy Landscapes, Lecture Notes in Physics*, edited by W. Janke (Springer, Heidelberg, 2007), pp. 67–106.
[31] O. Melchert and A. K. Hartmann, New J. Phys. **10**, 043039 (2008).
[32] C. Amoruso and A. K. Hartmann, Phys. Rev. B **70**, 134425 (2004).
[33] W. L. McMillan, Phys. Rev. B **29**, 4026 (1984).
[34] K. Binder, Z. Phys. B: Condens. Matter Quanta **43**, 119 (1981).
[35] J. Cardy, *Finite-Size Scaling* (Elsevier, Amsterdam, 1988).
[36] O. Melchert, arXiv:0910.5403.
[37] O. Melchert and A. K. Hartmann, Phys. Rev. B **76**, 174411 (2007).
[38] O. Melchert and A. K. Hartmann, Phys. Rev. B **79**, 184402 (2009).
[39] A. K. Hartmann, A. J. Bray, A. C. Carter, M. A. Moore, and A. P. Young, Phys. Rev. B **66**, 224401 (2002).
[40] A. K. Hartmann, Phys. Rev. E **60**, 5135 (1999).
[41] S. Boettcher, Eur. Phys. J. B **38**, 83 (2004).
[42] S. Boettcher, Phys. Rev. Lett. **95**, 197205 (2005).